Photochemical & Photobiological Sciences

PAPER

View Article Online
View Journal | View Issue

Cite this: *Photochem. Photobiol. Sci.*, 2014, **13**, 1297

Excited state proton transfer of 2-(2′-hydroxyphenyl)benzimidazole and its nitrogen substituted analogues in bovine serum albumin†

Francis A. S. Chipem, Santosh Kumar Behera and G. Krishnamoorthy*

Received 22nd March 2014,
Accepted 21st June 2014

DOI: 10.1039/c4pp00099d

www.rsc.org/pps

The interaction of 2-(2′-hydroxyphenyl)benzimidazole (HPBI) and its nitrogen substituted analogues 2-(2′-hydroxyphenyl)-3*H*-imidazo[4,5-*b*]pyridine (HPIP-b) and 2-(2′-hydroxyphenyl)-1*H*-imidazo-[4,5-*c*]-pyridine (HPIP-c) with BSA was explored. Upon interaction with BSA both normal and tautomer emissions are significantly enhanced. However, the fluorescence ratios of the normal band to the tautomer band of HPBI and HPIP-b decrease, but that of HPIP-c increases. From the tautomer emission, the stoichiometry and association constants were determined. HPBI exists as *cis*- and *trans*-enolic and zwitterionic forms, whereas HPIP-b and HPIP-c are present as monoanions in addition to *cis*- and *trans*-enols. The study shows that different conformers of all three molecules bind at different binding sites of BSA.

1. Introduction

Serum albumin is the most abundant protein found in blood plasma of the circulatory system. It has the ability to bind with extremely different types of compounds and is important in separation and drug delivery methods.[1–3] Serum albumins are microheterogeneous structures and act as transport proteins for various exogenous and endogenous molecules in the body by hydrophobic, hydrophilic, and ionic interactions. Human serum albumin (HSA), bovine serum albumin (BSA), equine serum albumin and rat serum albumin are some of the widely studied albumins. BSA is a globular water-soluble protein. Since it exhibits high conformational adaptability to a number of ligands, it is used as a model in many physical and chemical studies.[4,5] Besides, BSA is readily available and is easy to be extracted. Because of its stability and reproducibility, it is ideal for use in the calibration of many biological assays.[6]

The tertiary structure of BSA is composed of three domains I, II, and III where each of them is composed of subdomains A and B.[2,7,8] Domains II and III share a common interface and because of that the binding of an external molecule to domain III occurs with the conformational change of domain II affecting the binding affinities. For many medium sized molecules the primary binding sites are located in the hydrophobic cavities of subdomains IIA and IIIA which are sometimes referred to as site I and site II, respectively. The binding site I is sometimes referred to as Sudlow's site I or the warfarin binding site while the binding site II is also known as Sudlow's site II or the binding site of ibuprofen. Being at the surface of BSA, subdomain IB is exposed to the solvent environment. Tryptophan-214 is located deep in a hydrophobic microenvironment in subdomain IIA.

The information obtained from the study of the interaction of proteins with ligands helps to infer about the forces involved and the topology of the binding sites of the protein analyzed.[7–9] This has been the main method applied in modern days for elucidation of the protein structure in solution. The molecular interactions are often monitored using optical techniques, mainly fluorescence spectroscopic techniques, as these methods are relatively easy to use, highly sensitive and versatile.[9,10] Fluorescent probes bound to proteins have been used extensively for characterizing the binding sites in such biomolecules.[9,11–16] In particular proton transfer probes, able to reveal the presence of proton donors or acceptors, have been employed to elucidate the binding interaction through the environmental factors affecting the prototropic processes.[17,18]

Fluorophores exhibiting excited state intramolecular proton transfer (ESIPT) have been the object of research interest for many photobiologists and photochemists.[19–22] The dual emission, large Stokes' shifts and photostability make these fluorophores highly attractive for molecular devices as well as for sensing and probing applications.[20–31] In most cases, these fluorophores are used as ratiometric fluorescent probes.[30–35] ESIPT exhibiting molecules can emit normal and tautomer emission originating from two different conformers. However,

Department of Chemistry, Indian Institute of Technology Guwahati, Guwahati 781 039, India. E-mail: gkrishna@iitg.ernet.in

†Electronic supplementary information (ESI) available. See DOI: 10.1039/c4pp00099d

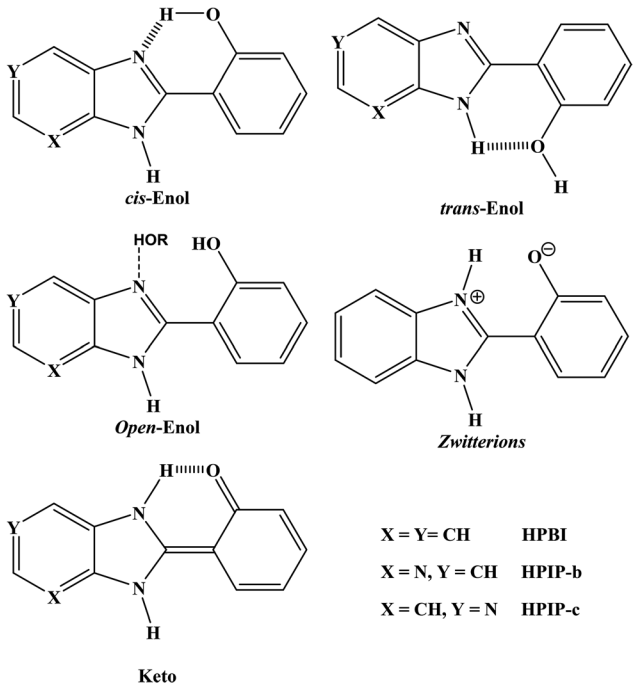

Chart 1 Different forms of HPBI and its nitrogen substituted molecules.

the presence of dual emission is strongly dependent on the environment. The ESIPT process and the characteristics of the fluorophore are strongly affected by the BSA environment also. Therefore, in recent years the photophysical studies of ESIPT molecules in BSA have gained attention.[36–39]

2-(2′-Hydroxyphenyl)benzimidazole (HPBI, Chart 1) and its analogues are some of the most extensively studied ESIPT molecules exhibiting normal and tautomer emissions.[19–22,40] HPBI has been applied as a fluorescent probe in various systems.[27–31] It is observed that the presence and the position of nitrogen substitution in benzimidazole and phenolic rings affects the spectral characteristics.[40–47] The quantum yield of the tautomer emission decreases on nitrogen substitution in the benzimidazole ring.[40–44] On the other hand, nitrogen substitution in the phenolic ring increases the quantum yield.[45,46] The decrease in the quantum yield of the tautomer emission has been ascribed to the nonradiative decay channel through the formation of an intramolecular charge transfer (ICT) state from the phototautomer.[44,47–53] Due to enhanced ICT and hydrogen bonding ability, the environmental sensitivity of the molecule increases with nitrogen substitution. Recently we have studied the effect of temperature,[51] metal ions[35] and β-cyclodextrin[29] on photophysical properties of HPBI and its nitrogen substituted analogues 2-(2′-hydroxyphenyl)-3*H*-imidazo[4,5-*b*]-pyridine (HPIP-b, Chart 1) and 2-(2′-hydroxyphenyl)-1*H*-imidazo-[4,5-*c*]pyridine (HPIP-c, Chart 1). Depending on the solvent, in the ground state, all three molecules exist in *cis*- and *trans*-enolic forms (Chart 1).[40–44,49] Upon photoexcitation, the *trans*-enol gives normal emission, but the *cis*-enol undergoes ESIPT to form a tautomer whose emission is largely Stokes shifted than the normal emission. In protic solvents, the intramolecular hydrogen bond of *cis*-enol can break to form open enol. Excitation of open enol also leads to normal emission. Here, we report the effect of the BSA environment on the characteristics of HPBI, HPIP-b and HPIP-c.

2. Materials and methods

The synthetic procedure for HPBI, HPIP-b and HPIP-c is reported elsewhere.[29] The ^{1}H-NMR, ^{13}C-NMR and FT-IR spectra of the synthesized compounds were given as supporting information elsewhere.[29] The compounds were recrystallized four times in methanol before use. BSA from Sigma Aldrich was used as received. The concentrations of the fluorophores in the solutions were maintained at ~5 μM. UV-visible absorption spectra were recorded using a Varian Cary 100 spectrophotometer. Fluorescence emission and excitation spectra were recorded using Edinburgh instrument FSP-920 and Horiba Jobin Yvon Fluoromax 4 fluorimeters.

3. Results and discussion

3.1. Photophysical characterization

Addition of BSA produces the hyperchromic effect in the absorption spectra of HPBI and HPIP-c (ESI, Fig. S1†). It exerts the hypochromic effect on the absorption spectra of HPIP-b. BSA induced spectral changes provide evidence for the interaction between the ligands and BSA. The different trend observed in HPIP-b with respect to HPBI and HPIP-c shows that the binding mode/binding site of HPIP-b is different from those of HPBI and HPIP-c.

All three fluorophores, HPBI, HPIP-b, and HPIP-c, display normal and tautomer emissions in aqueous solution (Fig. 1). The emission data observed are in agreement with the literature.[40,41,43] The tautomer emissions of HPBI and HPIP-c are more prominent than the normal emission and the intensity ratios of normal emission to tautomer emission are 0.19 and 0.17, respectively. But in the case of HPIP-b both bands are of nearly equal intensity and the ratio is 1.17. This shows that the relative population of *cis*-enol which is responsible for the tautomer emission is predominant in HPBI and HPIP-c. On the other hand, the relative population of *trans*-enol responsible for normal emission is little more than that of *cis*-enol in HPIP-b.

Upon addition of BSA, initially the intensities of both normal and tautomer emissions of HPBI decrease till 4 μM of BSA (Fig. 2a). With further addition of BSA, both emissions begin to increase. The saturation limit is observed at 48 μM of BSA. In BSA, the tautomer emission maximum is red shifted from 432 nm to 452 nm, whereas the emission maximum of normal emission is nearly unaffected.

As mentioned earlier, initially the normal band of HPIP-b was more prominent than the tautomer band, but as the concentration of BSA increases the tautomer band becomes more prominent (Fig. 2b). Up to 3.3 μM BSA, the intensity of the

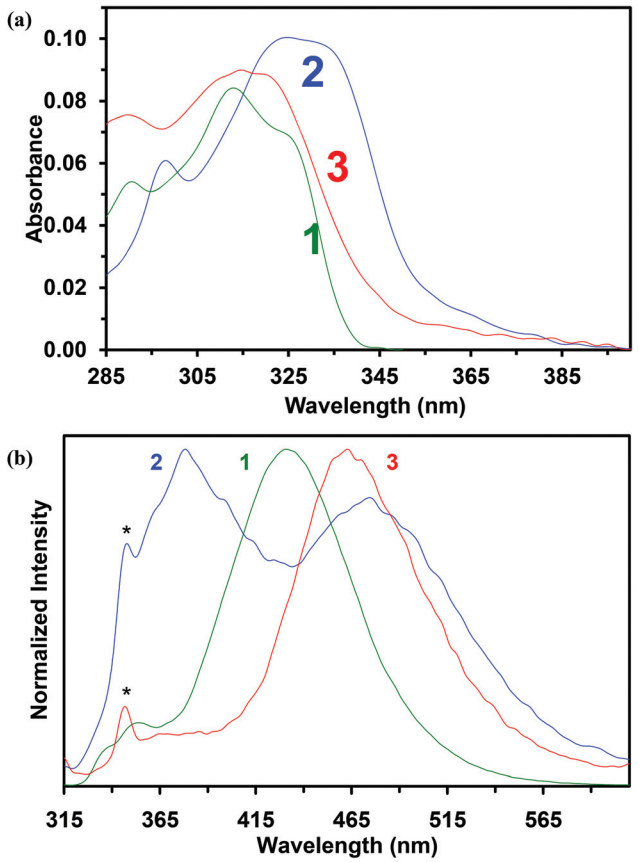

Fig. 1 (a) UV-Visible spectra and (b) normalized fluorescence spectra of (1) HPBI, (2) HPIP-b, and (3) HPIP-c in water at pH ~ 7.1 (λ_{exc} = 310 nm, water Raman peak is marked by *), at room temperature (298 ± 2 K). The concentration of the ligand is 5 μM.

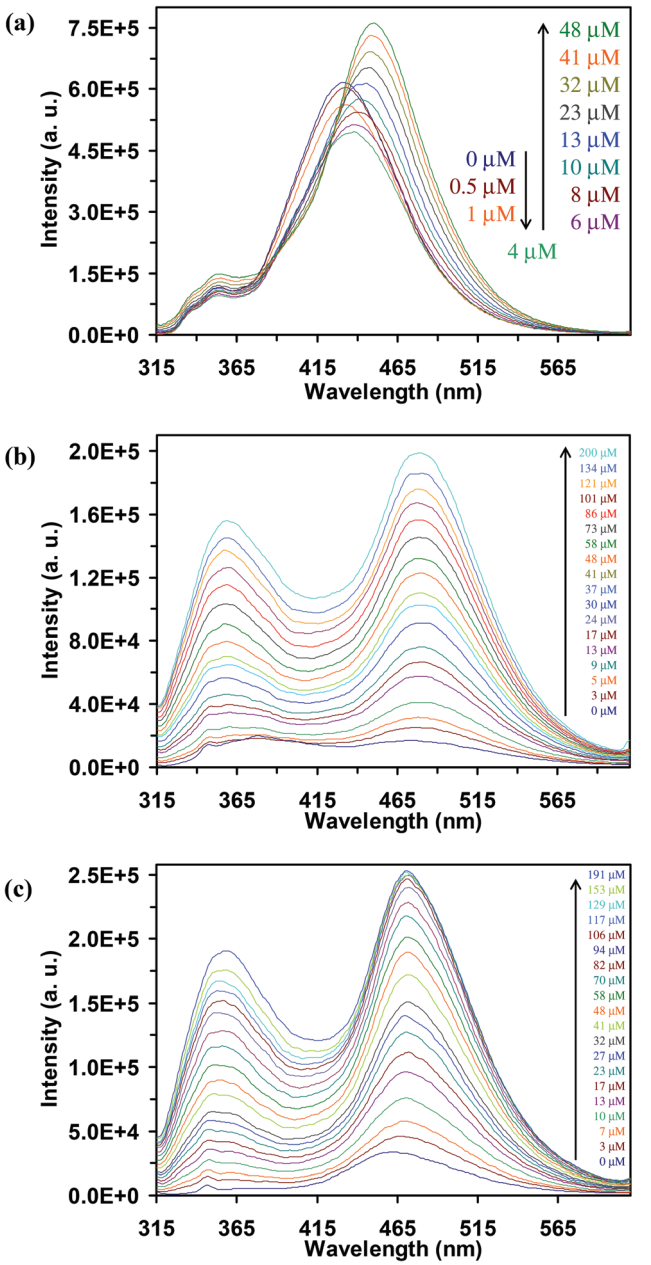

Fig. 2 Emission spectra of (a) HPBI, (b) HPIP-b, and (c) HPIP-c in the presence of BSA (λ_{exc} = 310 nm) at room temperature (298 ± 2 K). The concentration of the ligand is 5 μM.

normal band is marginally decreased and the emission maximum was blue shifted, but it increases with further addition of BSA. The normal band of HPIP-b is blue shifted from 378 nm in the absence of BSA to 360 nm in the presence of BSA. On the other hand, addition of BSA causes a small 4 nm red shift in the tautomer emission of HPIP-b.

In the case of HPIP-c, both normal and tautomer emissions gradually increase with increasing concentration of BSA (Fig. 2c). There is no change in the position of the normal band of HPIP-c upon binding with BSA, but the tautomer band is red-shifted from 463 nm in the absence of BSA to 471 nm at 200 μM of BSA.

Upon increasing the hydrophobicity of the environment, the tautomer emissions of HPBI and its nitrogen substituted analogues undergo a red shift and the normal emissions are blue shifted.[40–44,51] Such shifts in tautomer and normal emissions were also observed upon inclusion of these molecules into the hydrophobic β-cyclodextrin nanocavity.[29,54]

The red shift in the tautomer emissions suggests that in all cases the tautomer and its precursor *cis*-enol are in a hydrophobic environment. The very small red shift observed in the tautomer emission of HPIP-b suggests that its binding environment is less hydrophobic than that of HPBI and HPIP-c. In other words, the *cis*-enol of HPIP-b is more exposed to the solvent. On the other hand, the larger blue shift in the normal band of HPIP-b on increasing the concentration of BSA shows that the *trans*-enol of the HPIP-b molecule binds at a more hydrophobic site of the protein.

The intensity ratio of the normal band to the tautomer band gives a better picture on the effect of BSA on the *cis*-enol–*trans*-enol equilibrium. Fig. 3 shows the effect of BSA on the intensity ratio of three molecules. HPBI shows a small gradual decrease in the intensity ratio with the increase in concentration of BSA. The decrease in the intensity ratio is relatively

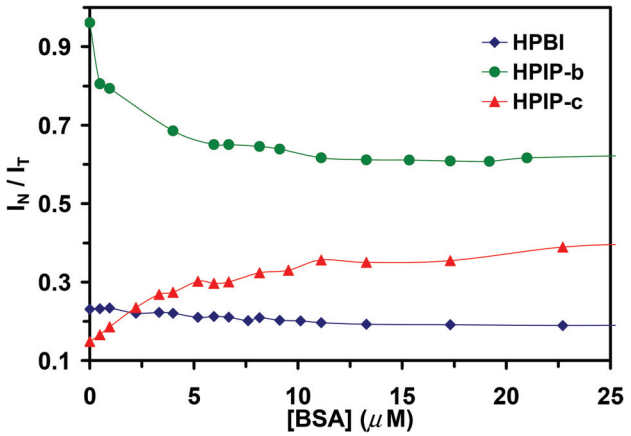

Fig. 3 Fluorescence intensity ratio plot of normal to tautomer bands of HPBI (♦), HPIP-b (●) and HPIP-c (▲) against the concentration of BSA at room temperature (298 ± 2 K). The wavelengths used in the measurements for HPBI, HPIP-b and HPIP-c are I_{355}/I_{452}, I_{360}/I_{478} and I_{360}/I_{471}, respectively.

more in HPIP-b up to the 1 : 1 ratio. In HPIP-b, beyond the 1 : 1 concentration ratio, the decrease in the intensity ratio of normal to tautomer bands becomes less. This decrease in the ratio in HPBI and HPIP-b shows that the tautomer emission becomes more prominent with an increase in the concentration of BSA. The increase in the tautomer emission may be due to two main factors: (i) the decrease in nonradiative deactivation of the phototautomer that occurs through the torsional rotation of the two aromatic rings that leads to the ICT state[44,47] and (ii) shifting of equilibrium in BSA towards the *cis*-enol conformer which is the ground state precursor of the phototautomer. However, in the case of HPIP-c the ratio increases with a positive slope upon an increase in the concentration of BSA. This shows that with an increase in the concentration of BSA the normal emission becomes more prominent than the tautomer emission. This increase in the intensity ratio of HPIP-c indicates that breaking of the intramolecular hydrogen bonded ring to form *trans*-enol is facilitated in BSA. This may be due to preferential hydrogen bonding of the probe molecule with amino acid residues bearing proton donor or acceptor groups. In other words, in contrast to the case of HPBI and HPIP-b, in HPIP-c the *cis*-enol-to-*trans*-enol equilibrium seems to be shifted towards *trans*-enol in BSA. This was further substantiated by the excitation spectra of the normal fluorescence, whose intensity dependence on the BSA concentration appears differentiated in the three molecules (ESI, Fig. S2†). In this context it is worth noting that in cyclodextrin where the binding site is the same, the equilibrium was shifted towards *cis*-enol in all cases.[29,54]

The excitation spectra of HPBI monitored at the tautomer band are different from those of HPIP-b and HPIP-c in the sense that for the initial addition of BSA up to 2.2 μM, the intensity of the band in HPBI decreases (Fig. 4a). On further addition of BSA, the intensity increases with an increase in BSA concentration. However, the fluorescence excitation spectral intensities of HPIP-b and HPIP-c gradually increase with

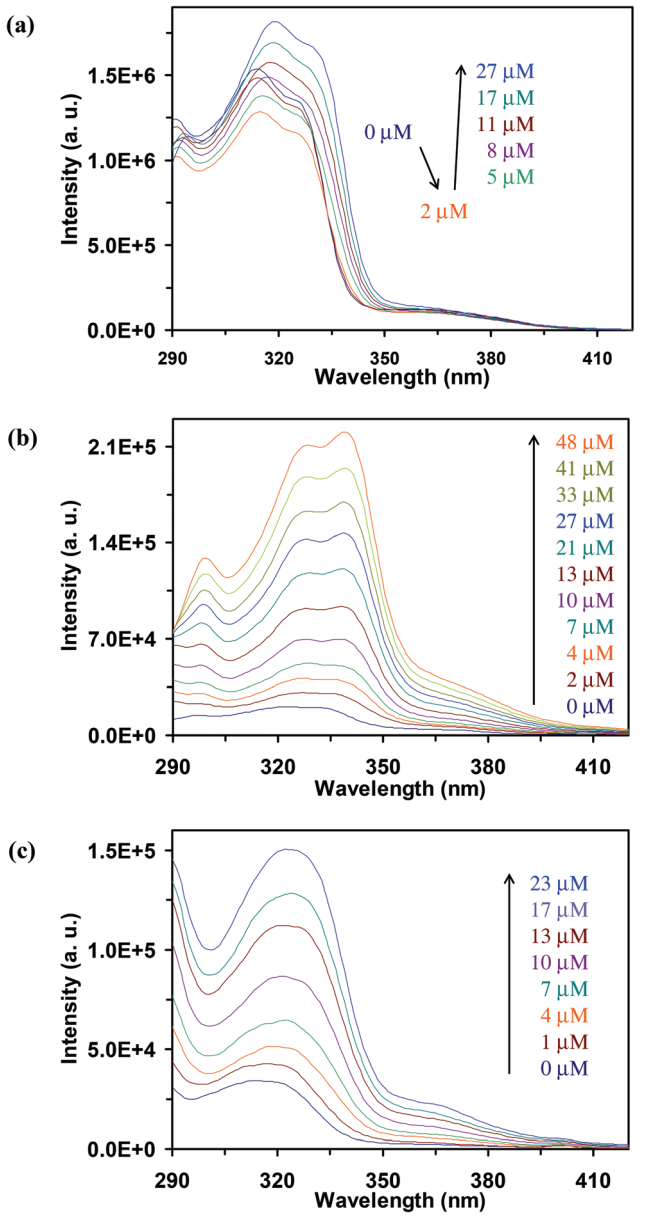

Fig. 4 Fluorescence excitation spectra of (a) HPBI (λ_{em} = 440 nm), (b) HPIP-b (λ_{em} = 460 nm), and (c) HPIP-c (λ_{em} = 440 nm) in the presence of BSA at room temperature (298 ± 2 K). The concentration of the ligand is 5 μM.

an increase in BSA concentration (Fig. 4b and c). Even in the absence of BSA the excitation spectra of HPBI has a shoulder at ~360 nm (Fig. 4a). Only a very little change is observed in the band upon increasing the concentrations of BSA. On the other hand in the other two derivatives only weak tails are observed at 350 nm in the absence of BSA (Fig. 4b and c). They gain intensity with addition of BSA.

As the main excitation band is due to *cis*-enol, to understand the red end shoulder the fluorescence spectra were obtained by excitation at the red end shoulder (Fig. 5). HPBI has an emission band at 440 nm in water and the band is blue shifted with an increase in BSA concentration. On the other

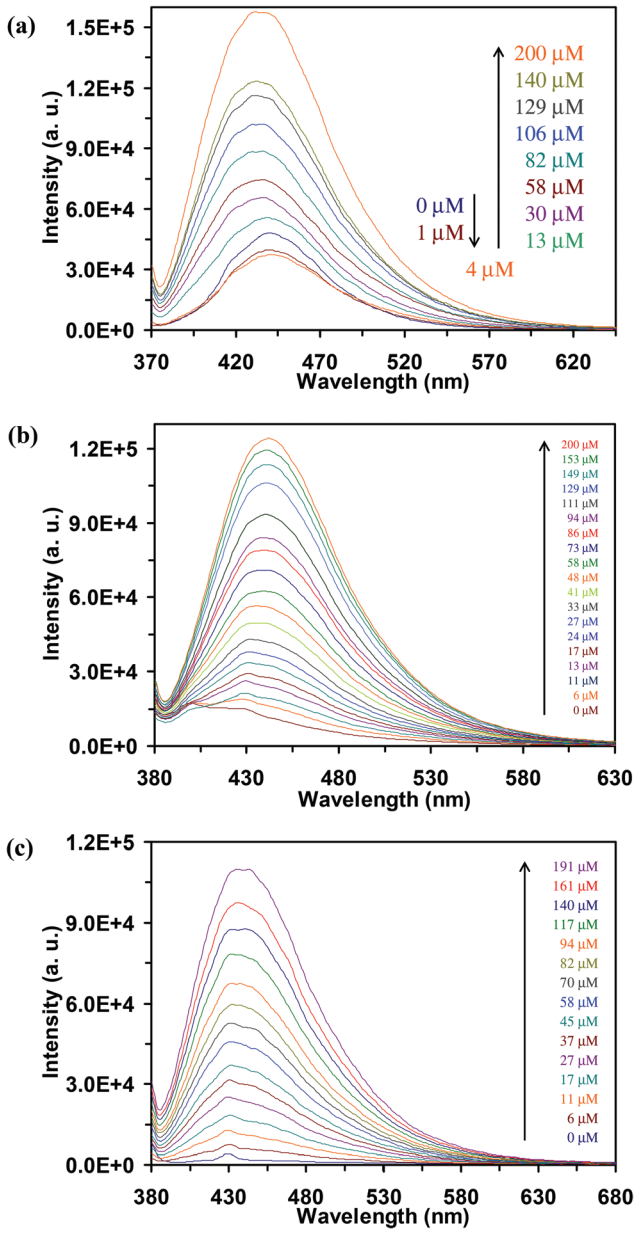

Fig. 5 Fluorescence spectra of (a) HPBI (λ_{exc} = 365 nm), (b) HPIP-b (λ_{exc} = 375 nm), and (c) HPIP-c (λ_{exc} = 375 nm) in the presence of BSA at room temperature (298 ± 2 K). The concentration of the ligand is 5 μM.

hand, addition of BSA shifts the emission maximum of HPIP-b to the red side and a new band appears at 443 nm and its intensity enhances with an increase in BSA quantity. In HPIP-c, only very weak emission is observed in the absence of BSA and a band emerges with addition of BSA and its intensity increases with further addition of BSA. All these indicate the presence of species other than two enolic forms in BSA.

The red side excitation bands and the corresponding fluorescence bands in HPBI can be assigned to zwitterions, and in HPIP-b and HPIP-c they can be assigned to the corresponding monoanions. These assignments are based on the following facts: (i) the red side fluorescence spectral band maximum

Table 1 Fluorescence excitation (λ_{max}^{exc} nm) and emission (λ_{max}^{fl} nm) band maxima of the red shifted band

Solution	λ_{max}^{exc}	λ_{max}^{fl}
HPBI		
Water	362	441
BSA (27 μM)	360	440
Monoanion (in water)[a]	304, 228	410
Zwitterion[a]		440
HPIP-b		
Water	—	—
BSA (48 μM)	365	443
Monoanion (in water)[b]	360	461
Monoanion (in DMSO)[b]	369	421
HPIP-c		
Water	—	—
BSA (23 μM)	366	439
Monoanion (in water)[b]	351	438
Monoanion (in DMSO)[b]	363	433

[a] Ref. 40. [b] Ref. 29.

(440 nm) is red shifted compared to the monoanion of HPBI (Table 1). (ii) Dogra *et al.* reported the formation of zwitterions in aqueous medium at pH 6,[40] and the fluorescence maximum of the observed zwitterions is in good agreement with that of the fluorescence spectrum obtained by excitation at 365 nm (Table 1). (iii) The formation of zwitterions was not observed for pyridyl nitrogen substituted analogues in any environment.[41–43] (iv) The pK_a value for neutral-monoanion equilibrium of HPBI is very high (~10), whereas those of HPIP-b (8.6) and HPIP-c (9.3) are relatively small. The pK_a value is expected to decrease inside the protein, due to the interaction of the phenolic –OH group with amino acid residues of proteins, as observed in β-CD.[29] (v) The fluorescence excitation and emission spectral maxima of the red side band of HPIP-b and HPIP-c are also in reasonable agreement with those of the corresponding monoanions (Table 1). Small discrepancy in the excitation and emission spectral maxima may be due to the effect of the environment. No appreciable change observed in the ~360 nm band excitation spectra of HPBI shows that the zwitterionic form of HPBI is present in the free molecule, and does not complex appreciably with BSA (Fig. 4a). Such a low affinity of zwitterionic molecules for serum albumin has been observed in the case of quinolones at neutral pH.[55]

The effect of BSA on the equilibria of HPBI and its nitrogen substituted analogues is summarized in Scheme 1 and also in ESI with structures, Scheme S1.†

3.2. Binding constants

The association constants for the binding of the ligands with BSA were determined from the fluorescence emission data using the Benesi–Hildebrand equation (eqn (1)).[56]

$$\frac{1}{I - I_0} = \frac{1}{I_\infty - I_0} + \frac{1}{(I_\infty - I_0)K[\mathrm{BSA}]} \quad (1)$$

where I_0, I and I_∞ are emission intensities in the absence of BSA, at an intermediate BSA concentration and when the fluorophore binds completely at a BSA binding site, respectively, and

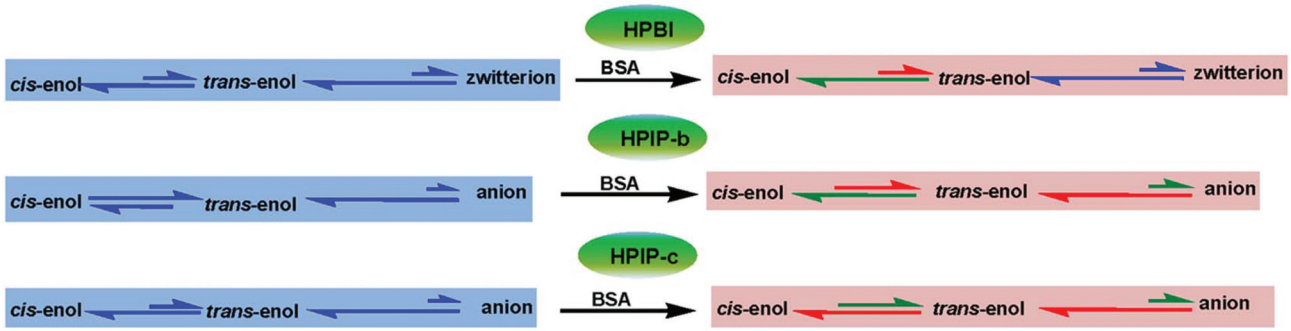

Scheme 1 Effect of BSA on the equilibrium.

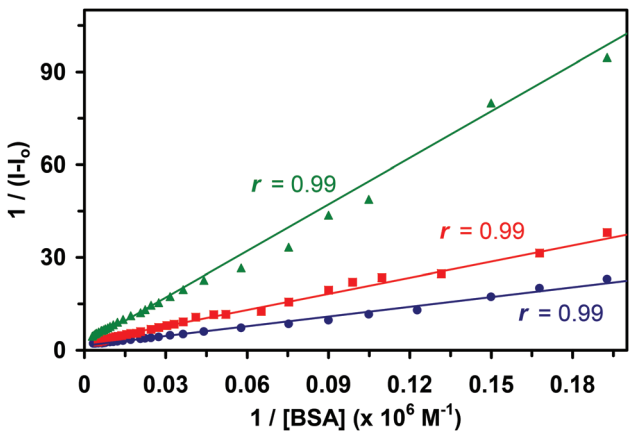

Fig. 6 Benesi–Hildebrand plot for HPBI (●), HPIP-b (■), and HPIP-c (▲) at room temperature (298 ± 2 K).

K is the association constant. The emission intensities of the tautomer emission at 455 nm, 484 nm and 472 nm are used for the Benesi–Hildebrand plot of HPBI, HPIP-b and HPIP-c, respectively. The Benesi–Hildebrand plots (Fig. 6) obtained with good linear correlations of $r = 0.99$ suggest that the inclusion complexes are predominantly 1 : 1 (fluorophore : BSA) in the represented protein concentration range. The plot was constructed starting from a BSA concentration of 4 μM. At lower concentrations the plot deviates from linearity due to multiple binding of different species in solution which can be located at different binding sites of BSA.

The binding constants of HPBI, HPIP-b and HPIP-c with the BSA protein are 14.3×10^3 M^{-1}, 14.9×10^3 M^{-1} and 4.0×10^3 M^{-1}, respectively. It is difficult to explain the trend in the binding constants due to the complexity of the binding process. However, possible arguments could be that HPBI is more hydrophobic than HPIP-c,[44] and hydrophobicity can control the binding of HPBI and HPIP-c, whereas hydrogen bonding plays a greater role in the binding of HPIP-b.

4. Conclusion

The interactions of the HPBI and its nitrogen substituted analogues with BSA are reported. All three fluorophores form 1 : 1 complexes with BSA. The fluorescence of both normal and tautomer bands increases substantially in BSA. On the other hand, the intensity ratios of normal to tautomer bands of HPBI and HPIP-b decrease, but that of HPIP-c increases in BSA. However, the tautomer emission is stronger than normal emission in all three molecules. The *cis*-enol of all three molecules binds at a hydrophobic site of BSA. The binding of *cis*-enol of HPIP-b is less hydrophobic than other molecules. On the other hand, as indicated by the larger shift, the *trans*-enol of HPIP-b binds at higher hydrophobic site. In addition to *cis*- and *trans*-enolic forms, HPBI is present in the zwitterionic form, whereas HPIP-b and HPIP-c are present as monoanions besides *cis*- and *trans*-enols in the ground state. In the excited state also along with tautomer and enol forms, HPBI and its pyridyl nitrogen analogues are present in the zwitterionic form and in the monoanionic form, respectively. While the monoanionic forms of HPIP-b and HPIP-c bind with BSA, the zwitterion of HPBI does not interact appreciably with the protein.

Acknowledgements

Department of Science and Technology (DST), New Delhi is acknowledged for the financial support. The authors acknowledge the Central Instruments Facility (CIF), IIT Guwahati for the Edinburgh instrument FSP-920.

References

1 A. A. Waheed, K. S. Rao and P. D. Gupta, Mechanism of dye binding in the protein assay using eosin dyes, *Anal. Biochem.*, 2000, **287**, 73–79.
2 X. M. He and D. C. Carter, Atomic-structure and chemistry of human serum-albumin, *Nature*, 1992, **358**, 209–215.
3 U. Kragh-Hansen, Molecular aspects of ligand binding to serum albumin, *Pharmacol. Rev.*, 1981, **33**, 17–53.
4 F. Karush, Heterogeneity of the binding sites of bovine serum albumin, *J. Am. Chem. Soc.*, 1950, **72**, 2705–2713.
5 P. Bourassa, C. D. Kanakis, P. Tarantilis, M. G. Pollissiou and H. A. Tajmir-Riahi, Resveratrol, genistein, and

curcumin bind bovine serum albumin, *J. Phys. Chem. B*, 2010, **114**, 3348–3354.
6 F.-L. Cui, J. Fan, J.-P. Lib and Z.-D. Hua, Interactions between 1-benzoyl-4-p-chlorophenyl thiosemicarbazide and serum albumin: Investigation by fluorescence spectroscopy, *Bioorg. Med. Chem.*, 2004, **12**, 151–157.
7 V. S. Jisha, K. T. Arun, M. Hariharan and D. Ramaiah, Site-selective binding and dual mode recognition of serum albumin by a squaraine dye, *J. Am. Chem. Soc.*, 2006, **128**, 6024–6025.
8 G. Sudlow, D. J. Birkett and D. N. Wade, Futher characterization of specifc drug binding-sites on human-serum albumin, *Mol. Pharmacol.*, 1976, **12**, 1052–1061.
9 J. R. Lakowicz, *Principles of Fluorescence Spectroscopy*, Springer, New York, 3rd edn, 2006.
10 A. J. Ozinskas, Principles of Fluorescence Immunoassay, in *Topics in Fluorescence Spectroscopy, Volume 4 – Probe Design and Chemical Sensing*, ed. J. R. Lakowicz, Plenum Press, New York and London, 1994, vol. 4, pp. 449–496.
11 H. Dodiuk, H. Kanety and E. M. Kosower, The apomyoglobin-a rylaminonaphthalenesulfonate system. Insight into fluorescent probe responses by substituent modulation, *J. Phys. Chem.*, 1979, **83**, 515–521.
12 B. K. Paul, A. Samanta and N. Guchhait, Exploring hydrophobic subdomain IIA of the protein bovine serum albumin in the native, intermediate, unfolded, and refolded States by a small fluorescence molecular reporter, *J. Phys. Chem. B*, 2010, **114**, 6183–6196.
13 B. K. Paul, D. Ray and N. Guchhait, Spectral deciphering of the interaction between intramolecular hydrogen bonded ESIPT drug, 3, 5-dichlorosalicylic acid, and a model transport protein, *Phys. Chem. Chem. Phys.*, 2012, **14**, 8892–8902.
14 L. Fabrizzi and A. Poggi, Sensors and switches from supramolecular chemistry, *Chem. Soc. Rev.*, 1995, **24**, 197–202.
15 B. Bhattacharya, S. Nakka, L. Guruprasad and A. Samanta, Interaction of bovine serum albumin with dipolar molecules: fluorescence and molecular docking Studies, *J. Phys. Chem. B*, 2009, **113**, 2143–2150.
16 P. T. Chou, W. C. Cooper and J. H. Clements, A comparative study. The photophysics of 2-phenylbenzoxazoles and 2-phenylbenzothiazoles, *Chem. Phys. Lett.*, 1993, **216**, 300–304.
17 B. K. Paul and N. Guchhait, Modulation of prototropic activity and rotational relaxation dynamics of a cationic biological photosensitizer within the motionally constrained bio-environment of a protein, *J. Phys. Chem. B*, 2011, **115**, 10322–10334.
18 M. R. Loken, J. W. Mayer, J. Gohlke and C. Brand, Excited-state proton transfer as a biological probe, Determination of rate constants by means of nanosecond fluorometry, *Biochemistry*, 1972, **11**, 4779–4786.
19 S. J. Formosinho and L. G. Arnaut, Excited- state proton-transfer reaction. 2. Intramolecular reactions, *J. Photochem. Photobiol., A*, 1993, **75**, 21–48.
20 J. E. Kwon and S. Y. Park, Advanced organic optoelectronic materials: Harnessing excited-state intramolecular proton transfer (ESIPT) process, *Adv. Mater.*, 2011, **23**, 3615–3642.
21 J. Zhao, S. Ji, Y. Chen, H. Guo and P. Yang, Excited state intramolecular proton transfer (ESIPT): From principal photophysics to the development of new chromophores and applications in fluorescent molecular probes and luminescent materials, *Phys. Chem. Chem. Phys.*, 2012, **14**, 8803–8817.
22 F. A. S. Chipem, A. Mishra and G. Krishnamoorthy, The role of hydrogen bonding in excited state intramolecular charge transfer, *Phys. Chem. Chem. Phys.*, 2012, **14**, 8775–8790.
23 J. Seo, S. Kim and S. Y. Park, Strong solvatochromic fluorescence from the Intramolecular charge-transfer state created by excited-state intramolecular proton transfer, *J. Am. Chem. Soc.*, 2004, **126**, 11154–11155.
24 Z. C. Wen, J. A. B. Ferreira and S. M. B. Costa, Novel pH tunable fluorescent sensor with dual recognition mode, *J. Photochem. Photobiol., A*, 2008, **199**, 98–104.
25 Q. Chou, D. A. Medvetz and Y. Pang, A polymeric colorimetric sensor with excited-state intramolecular proton transfer for anionic species, *Chem. Mater.*, 2007, **19**, 6421–6429.
26 M. Taki, J. L. Wolford and T. V. O'Halloran, Emission ratiometric imaging of intracellular zinc: design of a benzoxazole fluorescent sensor and its application in two-photon microscopy, *J. Am. Chem. Soc.*, 2004, **126**, 712–713.
27 S. K. Das, A. Bansal and S. K. Dogra, Excited state intramolecular proton transfer reactions in 2-(2-hydroxyphenyl)-benzimidazole in micellar solutions, *Bull. Chem. Soc. Jpn.*, 1997, **70**, 307–313.
28 A. L. Sobolewski, W. Domcke and C. Hättig, Photophysics of organic photostabilizers. Ab initio study of the excited-state deactivation mechanisms of 2-(2′-hydroxyphenyl)-benzotriazole, *J. Phys. Chem. A*, 2006, **110**, 6301–6306.
29 F. A. S. Chipem, S. K. Behera and G. Krishnamoorthy, Enhancing excited state intramolecular proton transfer in 2-(2′-hydroxyphenyl)benzimidazole and its nitrogen-substituted analogues by β-cyclodextrin: The effect of nitrogen substitution, *J. Phys. Chem. A*, 2013, **117**, 4084–4095.
30 N. Singh, N. Kaur, R. C. Mulrooney and J. F. Callan, A ratiometric fluorescent probe for magnesium employing excited state intramolecular proton transfer, *Tetrahedron Lett.*, 2008, **49**, 6690–6692.
31 C. Hou, Y. Xiong, N. Fu, C. C. Jacquot, T. C. Squier and H. Cao, Turn-on ratiometric fluorescent sensor for Pb^{2+} detection, *Tetrahedron Lett.*, 2011, **52**, 2692–2696.
32 R. Hu, J. Feng, D. Hu, S. Wang, S. Li, Y. Li and G. Yang, A rapid aqueous fluoride ion sensor with dual output modes, *Angew. Chem., Int. Ed.*, 2010, **49**, 4915–4918.
33 S. Banthia and A. Samanta, A new strategy for ratiometric fluorescence detection of transition metal ions, *J. Phys. Chem. B*, 2006, **110**, 6437–6440.
34 A. S. Klymchenko and A. P. Demchenko, Multiparametric probing of intermolecular interactions with fluorescent dye

exhibiting excited state intramolecular proton transfer, *Phys. Chem. Chem. Phys.*, 2003, **5**, 461–468.

35 F. A. S. Chipem, S. K. Behera and G. Krishnamoorthy, Ratiometric fluorescence sensing ability of 2-(2′-hydroxyphenyl)benzimidazole and its nitrogen substituted analogues towards metal ions, *Sens. Actuators, B*, 2014, **191**, 727–733.

36 F. S. Rodembusch, F. P. Leusin, L. F. D. Medina, A. Brandelli and V. Stefani, Synthesis and spectroscopic characterisation of new ESIPT fluorescent protein probes, *Photochem. Photobiol. Sci.*, 2005, **4**, 254–259.

37 D. Ray, B. K. Paul and N. Guchhait, Effect of biological confinement on the photophysics and dynamics of a proton-transfer phototautomer: an exploration of excitation and emission wavelength-dependent photophysics of the protein-bound drug, *Phys. Chem. Chem. Phys.*, 2012, **14**, 12182–12192.

38 B. K. Paul, D. Ray and N. Guchhait, Spectral deciphering of the interaction between an intramolecular hydrogen bonded ESIPT drug, 3,5-dichlorosalicylic acid, and a model transport protein, *Phys. Chem. Chem. Phys.*, 2012, **14**, 8892–8902.

39 M. G. Holler, L. F. Campo, A. Brandelli and V. Stefani, Synthesis and spectroscopic characterisation of 2-(2′-hydroxyphenyl)benzazole isothiocyanates as new fluorescent probes for proteins, *J. Photochem. Photobiol., A*, 2002, **149**, 217–225.

40 H. K. Sinha and S. K. Dogra, Ground and excited state prototropic reactions in 2-(ortho-hyroxyphenyl)benzimidazole, *Chem. Phys.*, 1986, **102**, 337–347.

41 G. Krishnamoorthy and S. K. Dogra, Prototropic reactions of 2(2′-hydroxyphenyl)-3H-imidazo[4,5-b]pyridine in aqueous and organic solvents, *J. Lumin.*, 2000, **92**, 103–114.

42 G. Krishnamoorthy and S. K. Dogra, Excited state intramolecular proton transfer in 2-(2′-hydroxyphenyl)-3H-imidazo[4,5-b]pyridine: effect of solvents, *J. Lumin.*, 2000, **92**, 91–102.

43 M. M. Balamurali and S. K. Dogra, Excited state intramolecular proton transfer in 2-(2′-hydroxyphenyl)-1H-imidazo-[4,5-c]pyridine: Effects of solvents, *J. Photochem. Photobiol., A*, 2002, **154**, 81–92.

44 F. A. S. Chipem and G. Krishnamoorthy, Comparative theoretical study of rotamerism and excited state intramolecular proton transfer of 2-(2′-hydroxyphenyl)benzimidazole, 2-(2′-hydroxyphenyl)imidazo[4,5-b]pyridine, 2-(2′-hydroxyphenyl)imidazo[4,5-c] pyridine and 8-(2′-hydroxyphenyl)purine, *J. Phys. Chem. A*, 2009, **113**, 12063–12070.

45 M. Mosquera, M. C. R. Rodríguez and F. Rodríguez-Prieto, Competition between protonation and deprotonation in the first excited singlet state of 2-(3′-hydroxy-2′-pyridyl)-benzimidazole in acidic solutions, *J. Phys. Chem. A*, 1997, **101**, 2766–2772.

46 M. C. R. Rodríguez, M. Mosquera and F. Rodríguez-Prieto, Ground- and excited-state tautomerism in anionic 2-(6′-hydroxy-2′-pyridyl)benzimidazole: Role of solvent and temperature, *J. Phys. Chem. A*, 2001, **105**, 10249–10260.

47 F. A. S. Chipem, N. Dash and G. Krishnamoorthy, Role of nitrogen substitution in phenyl ring on excited state intramolecular proton transfer and rotamerism of 2-(2′-hydroxyphenyl)benzimidazole: A theoretical study, *J. Chem. Phys.*, 2011, **134**, 104308.

48 D. LeGourriérec, V. Kharlanov, R. G. Brown and W. Rettig, Excited-state intramolecular proton transfer (ESIPT) in 2-(2′-hydroxyphenyl)-oxazole and –thiazole, *J. Photochem. Photobiol., A*, 2000, **130**, 101–111.

49 S. R. Vázquez, C. R. Rodríguez, M. Mosquera and F. Rodríguez-Prieto, Excited-state intramolecular proton transfer in 2-(3′-hydroxy-2′-pyridyl)benzoxazole. Evidence of coupled proton and charge transfer in the excited state of some o-hydroxyarylbenzazoles, *J. Phys. Chem. A*, 2007, **111**, 1814–1826.

50 V. A. Kharlanov, W. Rettig, M. I. Knyazhansky and N. Makaraova, Multiple emission of N-(1-anthryl)-pyridinium, *J. Photochem. Photobiol., A*, 1997, **103**, 45–50.

51 F. A. S. Chipem and G. Krishnamoorthy, Temperature effect on dual fluorescence of 2-(2′-Hydroxyphenyl)benzimidazole and its nitrogen substituted analogues, *J. Phys. Chem. B*, 2013, **117**, 14079–14088.

52 A. Brenlla, M. Veiga, M. C. R. Rodríguez, M. Mosquera and F. Rodríguez-Prieto, Fluorescence of methylated derivatives of hydroxyphenylimidazopyridine. Resolution of strongly overlapping spectra and a new ESIPT dye showing very efficient radiationless deactivation, *Photochem. Photobiol. Sci.*, 2011, **10**, 1622–1636.

53 H. Konoshima, S. Nagao, I. Kiyota, K. Amimoto, N. Yamamoto, M. Sekine, M. Nakata, K. Furukawa and H. Sekiya, Excited-state intramolecular proton transfer and charge transfer in 2-(2′-hydroxyphenyl)benzimidazole crystals studied by polymorphs-selected electronic spectroscopy, *Phys. Chem. Chem. Phys.*, 2012, **14**, 16448–16457.

54 E. L. Roberts, J. Dey and I. M. Warner, Excited-state intramolecular proton transfer of 2-(2′-hydroxyphenyl)-benzimidazole in cyclodextrins and binary solvent mixtures, *J. Phys. Chem. A*, 1997, **101**, 5296–5301.

55 F. Bosca, Seeking to shed some light on the binding of fluoroquinolones to albumins, *J. Phys. Chem. B*, 2012, **116**, 3504–3511.

56 M. L. Benesi and J. H. Hildebrand, A spectrophotometric investigation of the interaction of iodine with aromatic hydrocarbons, *J. Am. Chem. Soc.*, 1949, **71**, 2703–2707.

